Selection and characterization of a reovirus mutant with improved thermostability

Anthony J. Snyder[a] and Pranav Danthi[a#]

[a]Department of Biology, Indiana University, Bloomington, Indiana, USA

Running title: σ3 S344P alters properties of the reovirus capsid

[#]Corresponding author: Mailing address: Department of Biology, Indiana University, 212 S. Hawthorne Drive, Bloomington, IN 47405. Phone: (812) 856-2449. Fax: (812) 856-5710. E-mail: pdanthi@indiana.edu

ABSTRACT

The environment represents a significant barrier to infection. Physical stressors (heat) or chemical agents (ethanol and sodium dodecyl sulfate) can render virions noninfectious. As such, discrete proteins are necessary to stabilize the dual layered structure of mammalian orthoreovirus (reovirus). The outer capsid participates in cell entry: (i) σ3 is degraded to generate the infectious subviral particle and (ii) μ1 facilitates membrane penetration and subsequent core delivery. μ1-σ3 interactions also prevent inactivation; however, this activity is not fully characterized. Using forward and reverse genetic approaches, we identified two mutations (μ1 M258I and σ3 S344P) within heat resistant strains. σ3 S344P was sufficient to enhance capsid integrity and to reduce protease sensitivity. Moreover, these changes impaired replicative fitness in a reassortant background. This work reveals new details regarding the determinants of reovirus stability.

SIGNIFICANCE

Nonenveloped viruses rely on protein-protein interactions to shield their genomes from the environment. The capsid, or protective shell, must also disassemble during cell entry. In this work, we identified a determinant within mammalian orthoreovirus that regulates heat resistance, disassembly kinetics, and replicative fitness. Together, capsid function is balanced for optimal replication and for spread to a new host.

INTRODUCTION

Mammalian orthoreovirus (reovirus) is a versatile system to explore the properties of dual layered structures (1). Reovirus is composed of two concentric, protein shells (2). Each component serves a structural and/or functional role in the replication cycle. The inner capsid (core) encapsidates 10 segments of genomic dsRNA (1) and supports polymerase activity during infection (3-5). The core is highly stable, presumably to shield the viral genome from host sensors (6). The outer capsid comprises 200 μ1-σ3 heterohexamers and a maximum of 12 σ1 trimers (2, 7) and is required for cell entry (1). Virions are differentially sensitive to inactivating agents; μ1 adopts an altered conformation at elevated temperatures (6).

Reovirus initiates infection by attaching to proteinaceous receptors (8-10) or serotype-specific glycans (11-14). Virions are internalized by receptor-mediated endocytosis (15-18) and traffic to late endosomes (19-23). Acid dependent cathepsin proteases degrade σ3 (24-28) and cleave μ1 into μ1δ and Φ (Fig. 2A) (29). The resulting intermediate is called the infectious subviral particle (30). Proteolytic disassembly (virion-to-ISVP conversion) is recapitulated *in vitro* by treating purified virions with exogenous protease (29-31). During subsequent rearrangements (ISVP-to-ISVP* conversion), neighboring μ1 trimers separate (7, 32) and μ1δ is cleaved into μ1N and δ (Fig. 2A) (33, 34). The δ fragment then adopts a hydrophobic and protease sensitive conformation (35). This step is accompanied by the release of μ1N and Φ pore forming peptides, which disrupt the endosomal membrane (33-40). ISVP-to-ISVP* conversion can be triggered *in vitro* using heat (35, 41).

Reovirus must remain environmentally stable prior to infection. Heat or chemical agents render particles noninfectious (42, 43). Nonetheless, rare subpopulations harbor resistance-granting mutations, likely due to error prone replication. Studies of such variants provide clues regarding capsid stability and/or structure. When comparing prototype strains, differences in the efficiency of inactivation map to either the M2 gene segment (encodes for µ1) or the S4 gene segment (encodes for σ3) (35, 41, 43). µ1 mutations were selected by exposing virions to ethanol or by exposing ISVPs to heat. These changes reveal important µ1 mediated intratrimer, intertrimer, and trimer-core contacts (44-47). Similarly, σ3 Y354H was selected from persistently infected cells. This change alters capsid properties and allows for disassembly under limiting cathepsin activity (48, 49). σ3 also represents the primary determinant for virion thermostability (43). µ1-σ3 interactions are thought to prevent irreversible and premature, entry related conformational changes (6); however, this idea has not been fully investigated. In this work, we selected for and characterized heat resistant (HR) strains: (i) µ1 M258I and σ3 S344P were identified within HR strains, (ii) σ3 S344P was sufficient to enhance capsid integrity and to reduce protease sensitivity, and (iii) HR mutations impaired replicative fitness in a reassortant background.

MATERIALS AND METHODS

Cells and viruses. Murine L929 (L) cells were grown at 37°C in Joklik's minimal essential medium (Lonza) supplemented with 5% fetal bovine serum (Life Technologies), 2 mM L-glutamine (Invitrogen), 100 U/ml penicillin (Invitrogen), 100

115 µg/ml streptomycin (Invitrogen), and 25 ng/ml amphotericin B (Sigma-Aldrich). All
116 viruses used in this study were derived from reovirus type 1 Lang (T1L) and reovirus
117 type 3 Dearing (T3D) and were generated by plasmid-based reverse genetics (50, 51).
118 Mutations within the T1L S4, T1L M2, and T3D M2 genes were generated by
119 QuikChange site-directed mutagenesis (Agilent Technologies). S344P in T1L σ3 was
120 made using the following primer pair: forward 5'-
121 CTGCTCTCACAATGTTCCCGGACACCACCAAGTTCGG-3' and reverse 5'-
122 CCGAACTTGGTGGTGTCCGGGAACATTGTGAGAGCAG-3'. M258I in T1L µ1 was
123 made using the following primer pair: forward 5'-
124 TCAGAAGGAACTGTGATTAATGAGGCCGTGAATGC-3' and reverse 5'-
125 GCATTCACGGCCTCATTAATCACAGTTCCTTCTGA-3'. M258I in T3D µ1 was made
126 using the following primer pair: forward 5'-
127 ACGTATCAGAAGGCACCGTGATTAACGAGGCTGTC-3' and reverse 5'-
128 GACAGCCTCGTTAATCACGGTGCCTTCTGATACGT-3'.
129
130 **Virion purification.** Recombinant reoviruses T1L, T1L/T3D M2, T1L µ1 M258I, T1L σ3
131 S344P, T1L µ1 M258I σ3 S344P, and T1L/T3D M2 µ1 M258I σ3 S344P were
132 propagated and purified as previously described (50, 51). All variants in the T1L/T3D
133 M2 background contained a T3D M2 gene in an otherwise T1L background. L cells
134 infected with second passage reovirus stocks were lysed by sonication. Virions were
135 extracted from lysates using Vertrel-XF specialty fluid (Dupont) (52). The extracted
136 particles were layered onto 1.2- to 1.4-g/cm^3 CsCl step gradients. The gradients were
137 then centrifuged at 187,000×*g* for 4 h at 4°C. Bands corresponding to purified virions

(~1.36 g/cm^3) (53) were isolated and dialyzed into virus storage buffer (10 mM Tris, pH 7.4, 15 mM $MgCl_2$, and 150 mM NaCl). Following dialysis, the particle concentration was determined by measuring the optical density of the purified virion stocks at 260 nm (OD_{260}; 1 unit at OD_{260} = 2.1×10^{12} particles/ml) (54). The purification of virions was confirmed by SDS-PAGE and Coomassie brilliant blue (Sigma-Aldrich) staining.

Selection and isolation of heat resistant (HR) strains. T1L virions (2×10^{12} particles/ml) were incubated for 5 min at 55°C in a S1000 thermal cycler (Bio-Rad). The total volume of the reaction was 30 µl in virus storage buffer (10 mM Tris, pH 7.4, 15 mM $MgCl_2$, and 150 mM NaCl). Following incubation, 10 µl were analyzed by plaque assay. Putative HR strains were plaque purified at 5 days post infection. Next, L cell monolayers in 60 mm dishes (Greiner Bio-One) were adsorbed with the isolated plaques for 1 h at 4°C. Following the viral attachment incubation, the monolayers were washed three times with ice-cold PBS and overlaid with 2 ml of Joklik's minimal essential medium (Lonza) supplemented with 5% fetal bovine serum (Life Technologies), 2 mM L-glutamine (Invitrogen), 100 U/ml penicillin (Invitrogen), 100 µg/ml streptomycin (Invitrogen), and 25 ng/ml amphotericin B (Sigma-Aldrich). The cells were incubated at 37°C until cytopathic effect was observed and then lysed by two freeze-thaw cycles (first passage). To verify heat resistance, the infected cell lysates were incubated for 5 min at 55°C in a S1000 thermal cycler (Bio-Rad). The total volume of each reaction was 30 µl. For each isolate, an aliquot was also incubated for 5 min at 4°C. Following incubation, 10 µl of each reaction were diluted into 40 µl of ice-cold virus storage buffer (10 mM Tris, pH 7.4, 15 mM $MgCl_2$, and 150 mM NaCl) and infectivity

was determined by plaque assay. The change in infectivity was calculated using the following formula: $\log_{10}(\text{PFU/ml})_{55°C} - \log_{10}(\text{PFU/ml})_{4°C}$.

Sequencing of HR strains. L cell monolayers in 60 mm dishes (Greiner Bio-One) were adsorbed with first passage, verified HR strains for 1 h at 4°C. Following the viral attachment incubation, the monolayers were washed three times with ice-cold PBS and overlaid with 2 ml of Joklik's minimal essential medium (Lonza) supplemented with 5% fetal bovine serum (Life Technologies), 2 mM L-glutamine (Invitrogen), 100 U/ml penicillin (Invitrogen), 100 µg/ml streptomycin (Invitrogen), and 25 ng/ml amphotericin B (Sigma-Aldrich). At 24 h post infection, the cells were lysed with TRI Reagent (Molecular Research Center). Viral RNA was isolated by phenol-chloroform extraction and then subjected to reverse transcription (RT)-PCR using T1L S4 or T1L M2 gene segment-specific primers. PCR products were resolved on Tris-acetate-EDTA agarose gels, purified using a QIAquick gel extraction kit (Qiagen), and sequenced. The identified mutations were reintroduced into clean, T1L and T1L/T3D M2 backgrounds.

Sequence analysis. Multiple sequence alignments were created using the Clustal Omega program (55).

Structure analysis. Molecular graphics were created using the UCSF Chimera program (56).

Generation of infectious subviral particles (ISVPs). T1L, T1L/T3D M2, T1L μ1 M258I, T1L σ3 S344P, T1L μ1 M258I σ3 S344P, or T1L/T3D M2 μ1 M258I σ3 S344P virions (2×10^{12} particles/ml) were digested with 200 μg/ml TLCK (*N*α-*p*-tosyl-L-lysine chloromethyl ketone)-treated chymotrypsin (Worthington Biochemical) in a total volume of 100 μl for 20 min at 32°C (30, 31). The reactions were then incubated on ice for 20 min and quenched by the addition of 1 mM phenylmethylsulfonyl fluoride (PMSF) (Sigma-Aldrich). The generation of ISVPs was confirmed by SDS-PAGE and Coomassie brilliant blue (Sigma-Aldrich) staining.

Dynamic light scattering. T1L, T1L/T3D M2, T1L μ1 M258I, T1L σ3 S344P, T1L μ1 M258I σ3 S344P, or T1L/T3D M2 μ1 M258I σ3 S344P virions or ISVPs (2×10^{12} particles/ml) were analyzed using a Zetasizer Nano S dynamic light scattering system (Malvern Instruments). All measurements were made at room temperature in a quartz Suprasil cuvette with a 3.00-mm-path length (Hellma Analytics). For each sample, the size distribution profile was determined by averaging readings across 15 iterations.

Thermal inactivation and trypsin sensitivity assays. T1L, T1L/T3D M2, T1L μ1 M258I, T1L σ3 S344P, T1L μ1 M258I σ3 S344P, or T1L/T3D M2 μ1 M258I σ3 S344P virions or ISVPs (2×10^{12} particles/ml) were incubated for 5 min at the indicated temperatures in a S1000 thermal cycler (Bio-Rad). The total volume of each reaction was 30 μl in virus storage buffer (10 mM Tris, pH 7.4, 15 mM $MgCl_2$, and 150 mM NaCl). For each reaction condition, an aliquot was also incubated for 5 min at 4°C. Following incubation, 10 μl of each reaction were diluted into 40 μl of ice-cold virus

storage buffer (10 mM Tris, pH 7.4, 15 mM $MgCl_2$, and 150 mM NaCl) and infectivity was determined by plaque assay. The change in infectivity at a given temperature (*T*) was calculated using the following formula: $\log_{10}(PFU/ml)_T - \log_{10}(PFU/ml)_{4°C}$. The titers of the 4°C control samples were between 5×10^9 and 5×10^{10} PFU/ml. The remaining 20 µl of each reaction were either mock treated or treated with 0.08 mg/ml trypsin (Sigma-Aldrich) for 30 min on ice. Following digestion, equal particle numbers from each reaction were solubilized in reducing SDS sample buffer and analyzed by SDS-PAGE. The gels were Coomassie Brilliant Blue (Sigma-Aldrich) stained and imaged on an Odyssey imaging system (LI-COR).

Degradation of σ3 by exogenous protease. T1L, T1L/T3D M2, T1L µ1 M258I, T1L σ3 S344P, T1L µ1 M258I σ3 S344P, or T1L/T3D M2 µ1 M258I σ3 S344P virions (2×10^{12} particles/ml) were incubated in the presence of 10 µg/ml endoproteinase LysC (New England Biolabs) at 37°C in a S1000 thermal cycler (Bio-Rad). The starting volume of each reaction was 100 µl in virus storage buffer (10 mM Tris, pH 7.4, 15 mM $MgCl_2$, and 150 mM NaCl). At the indicated time points, 10 µl of each reaction was solubilized in reducing SDS sample buffer and boiled for 10 min at 95°C. Equal particle numbers from each time point were analyzed by SDS-PAGE. The gels were Coomassie Brilliant Blue (Sigma-Aldrich) stained and imaged on an Odyssey imaging system (LI-COR).

Ammonium chloride (AC) escape assay. L cell monolayers in 6-well plates (Greiner Bio-One) were adsorbed with T1L, T1L µ1 M258I, T1L σ3 S344P, or T1L µ1 M258I σ3

S344P virions (10 PFU/cell) for 1 h at 4°C. Following the viral attachment incubation, the monolayers were washed three times with ice-cold PBS and overlaid with 2 ml of Joklik's minimal essential medium (Lonza) supplemented with 5% fetal bovine serum (Life Technologies), 2 mM L-glutamine (Invitrogen), 100 U/ml penicillin (Invitrogen), 100 µg/ml streptomycin (Invitrogen), and 25 ng/ml amphotericin B (Sigma-Aldrich). The cells were either lysed immediately by two freeze-thaw cycles (input) or incubated at 37°C (start of infection). At the indicated times post infection, the growth medium was supplemented with 20 mM AC (Mallinckrodt Pharmaceuticals). At 24 h post infection, the cells were lysed by two freeze-thaw cycles and the virus titer was determined by plaque assay. The viral yield for each infection condition (timing of AC addition) (*t*) was calculated using the following formula: $\log_{10}(\text{PFU/ml})_t - \log_{10}(\text{PFU/ml})_{\text{input}}$. The titers of the input samples were between 1×10^5 and 4×10^5 PFU/ml.

Single- and multistep growth assays. L cell monolayers in 6-well plates (Greiner Bio-One) were adsorbed with T1L, T1L/T3D M2, T1L µ1 M258I, T1L σ3 S344P, T1L µ1 M258I σ3 S344P, or T1L/T3D M2 µ1 M258I σ3 S344P virions (10 PFU/cell or 0.01 PFU/cell) for 1 h at 4°C. Following the viral attachment incubation, the monolayers were washed three times with ice-cold PBS and overlaid with 2 ml of Joklik's minimal essential medium (Lonza) supplemented with 5% fetal bovine serum (Life Technologies), 2 mM L-glutamine (Invitrogen), 100 U/ml penicillin (Invitrogen), 100 µg/ml streptomycin (Invitrogen), and 25 ng/ml amphotericin B (Sigma-Aldrich). The cells were either lysed immediately by two freeze-thaw cycles (input) or incubated at 37°C (start of infection). At the indicated times post infection, the cells were lysed by

two freeze-thaw cycles and the virus titer was determined by plaque assay. The viral yield at a given time post infection (*t*) was calculated using the following formula: $\log_{10}(\text{PFU/ml})_t - \log_{10}(\text{PFU/ml})_{\text{input}}$. Following infection with 10 PFU/cell, the titers of the input samples were between 1×10^5 and 4×10^5 PFU/ml. Following infection with 0.01 PFU/cell, the titers of the input samples were between 1×10^2 and 3×10^2 PFU/ml.

Plaque assay. Control or heat-treated virus samples or infected cell lysates were diluted in PBS supplemented with 2 mM $MgCl_2$ (PBS^{Mg}). L cell monolayers in 6-well plates (Greiner Bio-One) were infected with 250 µl of diluted virus for 1 h at room temperature. Following the viral attachment incubation, the monolayers were overlaid with 4 ml of serum-free medium 199 (Sigma-Aldrich) supplemented with 1% Bacto Agar (BD Biosciences), 10 µg/ml TLCK-treated chymotrypsin (Worthington Biochemical), 2 mM L-glutamine (Invitrogen), 100 U/ml penicillin (Invitrogen), 100 µg/ml streptomycin (Invitrogen), and 25 ng/ml amphotericin B (Sigma-Aldrich). The infected cells were incubated at 37°C, and plaques were counted at 5 days post infection.

Statistical analysis. Unless noted otherwise, the reported values represent the mean of three independent, biological replicates. Error bars indicate standard deviation. *P* values were calculated using Student's *t* test (two-tailed, unequal variance assumed). For thermal inactivation experiments (Figs. 1A, 3A, and 5C), two criteria were used to assign significance: $P \leq 0.05$ and difference in change in infectivity ≥ 2 $\log_{10}$ units. For single- and multistep growth experiments (Fig. 6), two criteria were used to assign significance: $P \leq 0.05$ and difference in viral yield ≥ 1 $\log_{10}$ unit.

RESULTS AND DISCUSSION

Characterization of putative heat resistant (HR) strains. Reovirus is susceptible to environmental factors (42, 43). The loss of infectivity is correlated with outer capsid rearrangements (6, 35, 41). To isolate HR strains, type 1 Lang (T1L) virions were incubated at 55°C. The virus titer decreased by ~5.5 $\log_{10}$ units compared to the input (data not shown). Survivors were plaque purified and used to generate infected cell lysates. Three plaque isolates (out of 5) exhibited a bona fide HR phenotype (Fig. 1A). Sequencing of the μ1- and σ3-encoding gene segments (M2 and S4, respectively) revealed two mutations within each HR strain: μ1 M258I (conserved position) and σ3 S344P (nonconserved position) (Fig. 1B). These residues, which are not expected to interact, occupy distinct positions within the T1L μ1-σ3 heterohexamer (Figs. 1C-D) (7).

σ3 S344P was sufficient to enhance capsid integrity. Changes within other capsid components (σ1 and core proteins) could influence the HR phenotype. To address this concern, we reintroduced μ1 M258I and σ3 S344P into clean T1L backgrounds. Variants with one or both mutations displayed no observable defects in protein composition or protein stoichiometry. Due to autocatalytic activity, μ1 resolves as μ1C, and μ1δ resolves as δ (Figs. 2A-B) (33). We also analyzed virions and ISVPs by dynamic light scattering (DLS). In each case, we detected a single peak with no evidence of aggregation (Fig. 2C).

297 The S4 gene segment (encodes for σ3) contains the genetic determinants for
298 virion thermostability (43). σ3 preserves infectivity by stabilizing μ1 (6). Any change
299 that affects μ1-σ3 structure could modulate this activity. To test this idea, we performed
300 thermal inactivation experiments. Following incubation at 55°C, T1L and T1L μ1 M258I
301 virions were reduced in titer by ~5.5 $\log_{10}$ units relative to control that was incubated at
302 4°C. In contrast, T1L σ3 S344P and T1L μ1 M258I σ3 S344P virions were reduced in
303 titer by ~0.5 $\log_{10}$ units after incubation at 55°C and by ~4.0 $\log_{10}$ units after incubation
304 at 58°C (Fig. 3A). Virion associated μ1 adopts an ISVP*-like (protease sensitive)
305 conformation concurrent with inactivation. This transition is assayed *in vitro* by
306 determining the susceptibility of μ1 to trypsin digestion (6, 35, 41). Consistent with the
307 above results, 55°C was the minimal temperature at which μ1 in T1L and T1L μ1 M258I
308 virions became trypsin sensitive, whereas 58°C was the minimal temperature at which
309 μ1 in T1L σ3 S344P and T1L μ1 M258I σ3 S344P virions became trypsin sensitive (Fig.
310 3B). Of note, σ3 was absent from gels and μ1 migrated as uncleaved μ1C and cleaved
311 δ. Trypsin, which was used to probe for protease sensitivity, degrades σ3 and cleaves
312 at the μ1 δ-Φ junction (29). Heating alone was not sufficient to alter μ1 or σ3 levels
313 (Fig. 3C).
314 The M2 gene segment (encodes for μ1) contains the genetic determinants for
315 ISVP thermostability. The transition to ISVP* induces the loss of infectivity (35, 41).
316 Following incubation at 51°C, T1L, T1L μ1 M258I, T1L σ3 S344P, and T1L μ1 M258I σ3
317 S344P ISVPs were reduced in titer by ~5.0 $\log_{10}$ units (Fig. 3D). Thus, HR mutations
318 conferred stability only within the context of a virion (σ3 degradation restored wild-type-
319 like heat sensitivity). Protease treatment also serves as a biochemical probe for ISVP*

320 formation (35, 41). For each variant, δ (a product of μ1 cleavage) (Fig. 2A) became
321 trypsin sensitive at 51°C (Figs 3E). Heating alone was not sufficient to induce the loss
322 of δ (Fig. 3F).
323
324 **σ3 S344P was sufficient to reduce protease sensitivity.** Proteolytic disassembly
325 (virion-to-ISVP conversion) is required for reovirus to establish an infection (27). T1L is
326 more protease sensitive than T3D. This difference was mapped to polymorphisms at
327 344, 347, and 353 using recombinant protein (57). σ3 354 also regulates capsid
328 properties (48, 49). These residues are thought to influence conformational flexibility
329 through specific, intramonomer contacts (7, 57, 58). To determine if HR mutations alter
330 disassembly kinetics, virions were digested *in vitro* with endoproteinase LysC (EKC).
331 EKC probes for subtle differences in structure (57, 59). T1L and T1L μ1 M258I σ3 were
332 degraded within 40 min. In contrast, T1L σ3 S344P and T1L μ1 M258I σ3 S344P σ3
333 persisted (in part) for 100 min (Fig. 4A). We next tested the sensitivity to intracellular
334 proteases. Cathepsin B-L require endosomal acidification for activity. As such,
335 lysosomotropic weak bases (ammonium chloride [AC]) block infection (27, 60). Murine
336 L929 (L) cells were adsorbed with virions, and viral yield was quantified at 24 h post
337 infection. When indicated, the growth medium was supplemented with AC. The timing
338 of AC escape is related to the rate of disassembly (27). Consistent with the above
339 results, T1L and T1L μ1 M258I bypassed the block to infection with faster kinetics (viral
340 yield of ~1.5 $\log_{10}$ units when AC was added at 60 min) than T1L σ3 S344P and T1L μ1
341 M258I σ3 S344P (viral yield of ~1.5 $\log_{10}$ units when AC was added at 90 min) (Fig. 4B).
342 These results provide evidence that HR mutations diminish conformational flexibility;

343 enhanced capsid integrity (Fig. 3) was correlated with reduced protease sensitivity (Fig.
344 4). σ3 is initially cleaved in a hypersensitive region between 208-214 or 238-250 (57).
345 Presumably, σ3 S344P influenced protease accessibility. This idea was previously
346 suggested for σ3 Y354H (49). Of note, we did not observe a phenotype for μ1 M258I.
347 This change was identified within each HR strain; however, its function was not
348 determined.
349
350 **HR mutations altered capsid properties in a reassortant background.** T1L×T3D
351 reassortants are used extensively to study many aspects of the viral replication cycle
352 (1). For example, T1L/T3D M2 contains mismatched subunits (μ1-σ3 and μ1-core are
353 derived from different strains). Virions with imperfect interactions retain wild-type-like
354 stability and structure (6); however, HR mutations could function in a background
355 dependent manner. To address this question, we generated T1L/T3D M2 μ1 M258I σ3
356 S344P. This virus displayed no observable defects in protein composition, protein
357 stoichiometry, or particle size distribution (Figs. 5A-B). We next tested the impact on
358 capsid properties. Following incubation at 55°C, T1L/T3D M2 virions were reduced in
359 titer by ~5.5 $\log_{10}$ units, whereas T1L/T3D M2 μ1 M258I σ3 S344P virions were reduced
360 in titer by ~1.0 $\log_{10}$ unit. In contrast, ISVPs were equally thermostable (Fig. 5C). HR
361 mutations also conferred differential sensitivity to EKC. T1L/T3D M2 σ3 was degraded
362 within 40 min, whereas T1L/T3D M2 μ1 M258I σ3 S344P σ3 persisted (in part) for 100
363 min (Fig. 5D).
364

HR mutations impaired replicative fitness in a reassortant background. Reovirus disassembles efficiently during cell entry, yet remains stable in the environment. This balance is necessary for a productive infection and for spread to a new host (1, 61). HR mutations are favored at high temperatures (Figs. 3 and 5). We next examined their impact under physiological conditions. L cells were infected at high (10 PFU/cell) or low (0.01 PFU/cell) MOI, and viral yield was quantified at the indicated times post infection. Each T1L variant grew to similar levels (Fig. 6A). Thus, biochemical differences (described above) do not confer a selective advantage (or impediment) during a bona fide infection. In contrast, T1L/T3D M2 μ1 M258I σ3 S344P produced fewer infectious units than T1L/T3D M2 by 24 h post infection (high MOI) and by 48 and 72 h post infection (low MOI) (Fig. 6B). Interestingly, we attempted to isolate unique, HR strains in the reassortant background; however, each plaque isolate failed secondary screening (data not shown). The reduced viral yield and the absence (or low abundance) of resistant strains imply a replication defect.

Implications for host-pathogen interactions. The σ3 protein influences cell entry (24-28), particle assembly (62-67), and environmental stability (43). Moreover, differences in the efficiency of translational shutdown map to the S4 gene segment (encodes for σ3) (68). This effect may be direct or indirect by countering protein kinase R through σ3-dsRNA interactions (69, 70). σ3 function relies on its subcellular localization and its capacity to remain unbound from μ1; the affinity between μ1-σ3 varies based on strain (71). Thus, HR mutations could impact these activities in a

reassortant background. Mechanistic studies are needed to dissect the relationship between the host and hyperstable reovirus.

Conclusions. Resistance-granting mutations are tools to understand structure-function relationships, the basis (or mechanism) of inactivation, and replicative fitness. Toward this end, we selected for rare subpopulations at high temperatures (Figs. 1-2). HR strains contained two mutations within μ1-σ3. μ1 M258I was not associated with a phenotype, whereas σ3 S344P was sufficient to enhance capsid integrity and to reduce protease sensitivity (Figs. 3-4). Together, these changes impaired replicative fitness in a reassortant background (Fig. 6). This work reveals new details regarding the determinants of reovirus stability.

ACKNOWLEDGEMENTS

We thank members of our laboratory and the Indiana University virology community for helpful suggestions. Dynamic light scattering was performed in the Indiana University Physical Biochemistry Instrumentation Facility.

Research reported in this publication was supported by the National Institute of Allergy and Infectious Diseases of the National Institutes of Health under award numbers 1R01AI110637 (to P.D.) and F32AI126643 (to A.J.S.) and by Indiana University. The content is solely the responsibility of the authors and does not necessarily represent the official views of the funders.

REFERENCES

1. **Dermody T, Parker J, Sherry B.** 2013. Orthoreoviruses, Fields virology, vol 2. Lippincott Williams & Wilkins.

2. **Zhang X, Ji Y, Zhang L, Harrison SC, Marinescu DC, Nibert ML, Baker TS.** 2005. Features of reovirus outer capsid protein mu1 revealed by electron cryomicroscopy and image reconstruction of the virion at 7.0 Angstrom resolution. Structure **13:**1545-1557.

3. **Tao Y, Farsetta DL, Nibert ML, Harrison SC.** 2002. RNA synthesis in a cage--structural studies of reovirus polymerase lambda3. Cell **111:**733-745.

4. **Mertens P.** 2004. The dsRNA viruses. Virus Res **101:**3-13.

5. **Kumar CS, Dey D, Ghosh S, Banerjee M.** 2018. Breach: Host Membrane Penetration and Entry by Nonenveloped Viruses. Trends Microbiol **26:**525-537.

6. **Snyder AJ, Wang JC, Danthi P.** 2018. Components of the reovirus capsid differentially contribute to stability. J Virol doi:10.1128/JVI.01894-18.

7. **Liemann S, Chandran K, Baker TS, Nibert ML, Harrison SC.** 2002. Structure of the reovirus membrane-penetration protein, Mu1, in a complex with is protector protein, Sigma3. Cell **108:**283-295.

8. **Barton ES, Forrest JC, Connolly JL, Chappell JD, Liu Y, Schnell FJ, Nusrat A, Parkos CA, Dermody TS.** 2001. Junction adhesion molecule is a receptor for reovirus. Cell **104:**441-451.

9. **Campbell JA, Schelling P, Wetzel JD, Johnson EM, Forrest JC, Wilson GA, Aurrand-Lions M, Imhof BA, Stehle T, Dermody TS.** 2005. Junctional

433 adhesion molecule a serves as a receptor for prototype and field-isolate strains
434 of mammalian reovirus. J Virol **79:**7967-7978.
435 10. **Konopka-Anstadt JL, Mainou BA, Sutherland DM, Sekine Y, Strittmatter**
436 **SM, Dermody TS.** 2014. The Nogo receptor NgR1 mediates infection by
437 mammalian reovirus. Cell Host Microbe **15:**681-691.
438 11. **Gentsch JR, Pacitti AF.** 1985. Effect of neuraminidase treatment of cells and
439 effect of soluble glycoproteins on type 3 reovirus attachment to murine L cells. J
440 Virol **56:**356-364.
441 12. **Paul RW, Choi AH, Lee PW.** 1989. The alpha-anomeric form of sialic acid is
442 the minimal receptor determinant recognized by reovirus. Virology **172:**382-385.
443 13. **Reiss K, Stencel JE, Liu Y, Blaum BS, Reiter DM, Feizi T, Dermody TS,**
444 **Stehle T.** 2012. The GM2 glycan serves as a functional coreceptor for serotype
445 1 reovirus. PLoS Pathog **8:**e1003078.
446 14. **Reiter DM, Frierson JM, Halvorson EE, Kobayashi T, Dermody TS, Stehle**
447 **T.** 2011. Crystal structure of reovirus attachment protein sigma1 in complex with
448 sialylated oligosaccharides. PLoS Pathog **7:**e1002166.
449 15. **Borsa J, Morash BD, Sargent MD, Copps TP, Lievaart PA, Szekely JG.**
450 1979. Two modes of entry of reovirus particles into L cells. J Gen Virol **45:**161-
451 170.
452 16. **Ehrlich M, Boll W, Van Oijen A, Hariharan R, Chandran K, Nibert ML,**
453 **Kirchhausen T.** 2004. Endocytosis by random initiation and stabilization of
454 clathrin-coated pits. Cell **118:**591-605.

17. **Boulant S, Stanifer M, Kural C, Cureton DK, Massol R, Nibert ML, Kirchhausen T.** 2013. Similar uptake but different trafficking and escape routes of reovirus virions and infectious subvirion particles imaged in polarized Madin-Darby canine kidney cells. Mol Biol Cell **24:**1196-1207.

18. **Schulz WL, Haj AK, Schiff LA.** 2012. Reovirus uses multiple endocytic pathways for cell entry. J Virol **86:**12665-12675.

19. **Maginnis MS, Forrest JC, Kopecky-Bromberg SA, Dickeson SK, Santoro SA, Zutter MM, Nemerow GR, Bergelson JM, Dermody TS.** 2006. Beta1 integrin mediates internalization of mammalian reovirus. J Virol **80:**2760-2770.

20. **Maginnis MS, Mainou BA, Derdowski A, Johnson EM, Zent R, Dermody TS.** 2008. NPXY motifs in the beta1 integrin cytoplasmic tail are required for functional reovirus entry. J Virol **82:**3181-3191.

21. **Mainou BA, Dermody TS.** 2011. Src kinase mediates productive endocytic sorting of reovirus during cell entry. J Virol **85:**3203-3213.

22. **Mainou BA, Dermody TS.** 2012. Transport to late endosomes is required for efficient reovirus infection. J Virol **86:**8346-8358.

23. **Mainou BA, Zamora PF, Ashbrook AW, Dorset DC, Kim KS, Dermody TS.** 2013. Reovirus cell entry requires functional microtubules. MBio **4**.

24. **Baer GS, Dermody TS.** 1997. Mutations in reovirus outer-capsid protein sigma3 selected during persistent infections of L cells confer resistance to protease inhibitor E64. J Virol **71:**4921-4928.

476 25. **Borsa J, Sargent MD, Lievaart PA, Copps TP.** 1981. Reovirus: evidence for a
477 second step in the intracellular uncoating and transcriptase activation process.
478 Virology **111:**191-200.
479 26. **Ebert DH, Deussing J, Peters C, Dermody TS.** 2002. Cathepsin L and
480 cathepsin B mediate reovirus disassembly in murine fibroblast cells. J Biol
481 Chem **277:**24609-24617.
482 27. **Sturzenbecker LJ, Nibert M, Furlong D, Fields BN.** 1987. Intracellular
483 digestion of reovirus particles requires a low pH and is an essential step in the
484 viral infectious cycle. J Virol **61:**2351-2361.
485 28. **Silverstein SC, Astell C, Levin DH, Schonberg M, Acs G.** 1972. The
486 mechanisms of reovirus uncoating and gene activation in vivo. Virology **47:**797-
487 806.
488 29. **Nibert ML, Fields BN.** 1992. A carboxy-terminal fragment of protein mu 1/mu
489 1C is present in infectious subvirion particles of mammalian reoviruses and is
490 proposed to have a role in penetration. J Virol **66:**6408-6418.
491 30. **Borsa J, Copps TP, Sargent MD, Long DG, Chapman JD.** 1973. New
492 intermediate subviral particles in the in vitro uncoating of reovirus virions by
493 chymotrypsin. J Virol **11:**552-564.
494 31. **Joklik WK.** 1972. Studies on the effect of chymotrypsin on reovirions. Virology
495 **49:**700-715.
496 32. **Zhang L, Chandran K, Nibert ML, Harrison SC.** 2006. Reovirus mu1
497 structural rearrangements that mediate membrane penetration. J Virol
498 **80:**12367-12376.

499 33. **Nibert ML, Odegard AL, Agosto MA, Chandran K, Schiff LA.** 2005. Putative
500 autocleavage of reovirus mu1 protein in concert with outer-capsid disassembly
501 and activation for membrane permeabilization. J Mol Biol **345:**461-474.
502 34. **Odegard AL, Chandran K, Zhang X, Parker JS, Baker TS, Nibert ML.** 2004.
503 Putative autocleavage of outer capsid protein micro1, allowing release of
504 myristoylated peptide micro1N during particle uncoating, is critical for cell entry
505 by reovirus. J Virol **78:**8732-8745.
506 35. **Chandran K, Farsetta DL, Nibert ML.** 2002. Strategy for nonenveloped virus
507 entry: a hydrophobic conformer of the reovirus membrane penetration protein
508 micro 1 mediates membrane disruption. J Virol **76:**9920-9933.
509 36. **Agosto MA, Ivanovic T, Nibert ML.** 2006. Mammalian reovirus, a
510 nonfusogenic nonenveloped virus, forms size-selective pores in a model
511 membrane. Proc Natl Acad Sci U S A **103:**16496-16501.
512 37. **Ivanovic T, Agosto MA, Zhang L, Chandran K, Harrison SC, Nibert ML.**
513 2008. Peptides released from reovirus outer capsid form membrane pores that
514 recruit virus particles. EMBO J **27:**1289-1298.
515 38. **Nibert ML, Schiff LA, Fields BN.** 1991. Mammalian reoviruses contain a
516 myristoylated structural protein. J Virol **65:**1960-1967.
517 39. **Snyder AJ, Danthi P.** 2018. Cleavage of the C-Terminal Fragment of Reovirus
518 mu1 Is Required for Optimal Infectivity. J Virol **92**.
519 40. **Zhang L, Agosto MA, Ivanovic T, King DS, Nibert ML, Harrison SC.** 2009.
520 Requirements for the formation of membrane pores by the reovirus
521 myristoylated micro1N peptide. J Virol **83:**7004-7014.

522 41. **Middleton JK, Severson TF, Chandran K, Gillian AL, Yin J, Nibert ML.**
523 2002. Thermostability of reovirus disassembly intermediates (ISVPs) correlates
524 with genetic, biochemical, and thermodynamic properties of major surface
525 protein mu1. J Virol **76:**1051-1061.
526 42. **Drayna D, Fields BN.** 1982. Biochemical studies on the mechanism of
527 chemical and physical inactivation of reovirus. J Gen Virol **63 (Pt 1):**161-170.
528 43. **Drayna D, Fields BN.** 1982. Genetic studies on the mechanism of chemical
529 and physical inactivation of reovirus. J Gen Virol **63 (Pt 1):**149-159.
530 44. **Agosto MA, Middleton JK, Freimont EC, Yin J, Nibert ML.** 2007.
531 Thermolabilizing pseudoreversions in reovirus outer-capsid protein micro 1
532 rescue the entry defect conferred by a thermostabilizing mutation. J Virol
533 **81:**7400-7409.
534 45. **Hooper JW, Fields BN.** 1996. Role of the mu 1 protein in reovirus stability and
535 capacity to cause chromium release from host cells. J Virol **70:**459-467.
536 46. **Middleton JK, Agosto MA, Severson TF, Yin J, Nibert ML.** 2007.
537 Thermostabilizing mutations in reovirus outer-capsid protein mu1 selected by
538 heat inactivation of infectious subvirion particles. Virology **361:**412-425.
539 47. **Wessner DR, Fields BN.** 1993. Isolation and genetic characterization of
540 ethanol-resistant reovirus mutants. J Virol **67:**2442-2447.
541 48. **Wetzel JD, Wilson GJ, Baer GS, Dunnigan LR, Wright JP, Tang DS,**
542 **Dermody TS.** 1997. Reovirus variants selected during persistent infections of L
543 cells contain mutations in the viral S1 and S4 genes and are altered in viral
544 disassembly. Journal of virology **71:**1362-1369.

545 49. **Doyle JD, Danthi P, Kendall EA, Ooms LS, Wetzel JD, Dermody TS.** 2012.
546 Molecular determinants of proteolytic disassembly of the reovirus outer capsid.
547 J Biol Chem **287:**8029-8038.
548 50. **Berard A, Coombs KM.** 2009. Mammalian reoviruses: propagation,
549 quantification, and storage. Curr Protoc Microbiol **Chapter 15:**Unit15C 11.
550 51. **Kobayashi T, Ooms LS, Ikizler M, Chappell JD, Dermody TS.** 2010. An
551 improved reverse genetics system for mammalian orthoreoviruses. Virology
552 **398:**194-200.
553 52. **Mendez, II, Hermann LL, Hazelton PR, Coombs KM.** 2000. A comparative
554 analysis of freon substitutes in the purification of reovirus and calicivirus. J Virol
555 Methods **90:**59-67.
556 53. **Smith RE, Zweerink HJ, Joklik WK.** 1969. Polypeptide components of virions,
557 top component and cores of reovirus type 3. Virology **39:**791-810.
558 54. **Coombs KM.** 1998. Stoichiometry of reovirus structural proteins in virus, ISVP,
559 and core particles. Virology **243:**218-228.
560 55. **Sievers F, Wilm A, Dineen D, Gibson TJ, Karplus K, Li W, Lopez R,**
561 **McWilliam H, Remmert M, Soding J, Thompson JD, Higgins DG.** 2011.
562 Fast, scalable generation of high-quality protein multiple sequence alignments
563 using Clustal Omega. Mol Syst Biol **7:**539.
564 56. **Pettersen EF, Goddard TD, Huang CC, Couch GS, Greenblatt DM, Meng**
565 **EC, Ferrin TE.** 2004. UCSF Chimera--a visualization system for exploratory
566 research and analysis. J Comput Chem **25:**1605-1612.

567 57. **Jane-Valbuena J, Breun LA, Schiff LA, Nibert ML.** 2002. Sites and
568 determinants of early cleavages in the proteolytic processing pathway of
569 reovirus surface protein sigma3. J Virol **76:**5184-5197.
570 58. **Olland AM, Jane-Valbuena J, Schiff LA, Nibert ML, Harrison SC.** 2001.
571 Structure of the reovirus outer capsid and dsRNA-binding protein sigma3 at 1.8
572 A resolution. EMBO J **20:**979-989.
573 59. **Jane-Valbuena J, Nibert ML, Spencer SM, Walker SB, Baker TS, Chen Y,**
574 **Centonze VE, Schiff LA.** 1999. Reovirus virion-like particles obtained by
575 recoating infectious subvirion particles with baculovirus-expressed sigma3
576 protein: an approach for analyzing sigma3 functions during virus entry. J Virol
577 **73:**2963-2973.
578 60. **Rawlings ND, Salvesen G.** 2013. Handbook of proteolytic enzymes, Third
579 edition. / ed. Elsevier/AP, Amsterdam.
580 61. **Flint SJ, Racaniello VR, Rall GF, Skalka AM, Enquist LW.** 2015. Principles of
581 virology, 4th edition. ed. ASM Press, Washington, DC.
582 62. **Antczak JB, Joklik WK.** 1992. Reovirus genome segment assortment into
583 progeny genomes studied by the use of monoclonal antibodies directed against
584 reovirus proteins. Virology **187:**760-776.
585 63. **Danis C, Garzon S, Lemay G.** 1992. Further characterization of the ts453
586 mutant of mammalian orthoreovirus serotype 3 and nucleotide sequence of the
587 mutated S4 gene. Virology **190:**494-498.

64. **Mabrouk T, Lemay G.** 1994. The sequence similarity of reovirus sigma 3 protein to picornaviral proteases is unrelated to its role in mu 1 viral protein cleavage. Virology **202:**615-620.

65. **Morgan EM, Zweerink HJ.** 1974. Reovirus morphogenesis. Corelike particles in cells infected at 39 degrees with wild-type reovirus and temperature-sensitive mutants of groups B and G. Virology **59:**556-565.

66. **Roner MR, Lin PN, Nepluev I, Kong LJ, Joklik WK.** 1995. Identification of signals required for the insertion of heterologous genome segments into the reovirus genome. Proc Natl Acad Sci U S A **92:**12362-12366.

67. **Shing M, Coombs KM.** 1996. Assembly of the reovirus outer capsid requires mu 1/sigma 3 interactions which are prevented by misfolded sigma 3 protein in temperature-sensitive mutant tsG453. Virus Res **46:**19-29.

68. **Sharpe AH, Fields BN.** 1982. Reovirus inhibition of cellular RNA and protein synthesis: role of the S4 gene. Virology **122:**381-391.

69. **Denzler KL, Jacobs BL.** 1994. Site-directed mutagenic analysis of reovirus sigma 3 protein binding to dsRNA. Virology **204:**190-199.

70. **Yue Z, Shatkin AJ.** 1997. Double-stranded RNA-dependent protein kinase (PKR) is regulated by reovirus structural proteins. Virology **234:**364-371.

71. **Schmechel S, Chute M, Skinner P, Anderson R, Schiff L.** 1997. Preferential translation of reovirus mRNA by a sigma3-dependent mechanism. Virology **232:**62-73.

611 **FIGURE LEGENDS**

612 **FIG 1** Selection, isolation, and sequencing of heat resistant strains. (A) Thermal
613 inactivation. T1L virions were incubated for 5 min at 55°C. Surviving strains were
614 plaque purified and amplified on L cells. To verify heat resistance, the infected cell
615 lysates were incubated for 5 min at 55°C. The change in infectivity relative to samples
616 incubated at 4°C was determined by plaque assay. The data are presented as means ±
617 SDs. *, $P \leq 0.05$ and difference in change in infectivity ≥ 2 $\log_{10}$ units (n = 3
618 independent replicates). (B) Multiple sequence alignments. Residues corresponding to
619 μ1 258 and σ3 344 are in boldface. (C) Side view of the T1L μ1-σ3 heterohexamer (7)
620 (Protein Data Bank [PDB] accession number 1JMU). (D) Top and bottom views (left
621 and right, respectively) of the T1L μ1-σ3 heterohexamer (7) (Protein Data Bank [PDB]
622 accession number 1JMU). In panels C and D, μ1 monomers are colored blue, σ3
623 monomers are colored red, μ1 258 is represented by magenta spheres, and σ3 344 is
624 represented by green spheres.
625
626 **FIG 2** Protein compositions and size distribution profiles of T1L variants. (A) Schematic
627 of μ1 cleavage fragments. (B) Protein compositions. T1L, T1L μ1 M258I, T1L σ3
628 S344P, and T1L μ1 M258I σ3 S344P virions and ISVPs were analyzed by SDS-PAGE.
629 The gel was Coomassie brilliant blue stained. The migration of capsid proteins is
630 indicated on the left. μ1 resolves as μ1C, and μ1δ resolves as δ (33). μ1N and Φ are
631 too small to resolve on the gel (n = 3 independent replicates; results from 1
632 representative experiment are shown). (C) Size distribution profiles. T1L, T1L μ1
633 M258I, T1L σ3 S344P, or T1L μ1 M258I σ3 S344P virions or ISVPs were analyzed by

dynamic light scattering. For each variant, the virion (black) and ISVP (gray) size distribution profiles are overlaid (n = 3 independent replicates; results from 1 representative experiment are shown).

FIG 3 Thermostability of T1L variants. (A and D) Thermal inactivation. T1L, T1L μ1 M258I, T1L σ3 S344P, or T1L μ1 M258I σ3 S344P virions (A) or ISVPs (D) were incubated in virus storage for 5 min at the indicated temperatures. The change in infectivity relative to samples incubated at 4°C was determined by plaque assay. The data are presented as means ± SDs. *, $P \leq 0.05$ and difference in change in infectivity ≥ 2 $\log_{10}$ units (n = 3 independent replicates). (B and E) Heat induced conformational changes. T1L, T1L μ1 M258I, T1L σ3 S344P, or T1L μ1 M258I σ3 S344P virions (B) or ISVPs (E) were incubated in virus storage buffer for 5 min at the indicated temperatures. Each reaction was then treated with trypsin for 30 min on ice. Following digestion, equal particle numbers from each reaction were analyzed by SDS-PAGE. The gels were Coomassie brilliant blue stained (n = 3 independent replicates; results from 1 representative experiment are shown). (C and F). Composition of heated virus. T1L, T1L μ1 M258I, T1L σ3 S344P, or T1L μ1 M258I σ3 S344P virions (C) or ISVPs (F) were incubated in virus storage buffer for 5 min at the indicated temperatures. Equal particle numbers from each reaction were analyzed by SDS-PAGE. The gels were Coomassie brilliant blue stained (n = 3 independent replicates; results from 1 representative experiment are shown).

FIG 4 Degradation of σ3 by exogenous and intracellular proteases. (A) Exogenous protease. T1L, T1L μ1 M258I, T1L σ3 S344P, or T1L μ1 M258I σ3 S344P virions were incubated in virus storage buffer supplemented with endoproteinase LysC for the indicated amounts of time at 37°C. Following digestion, equal particle numbers from each time point were analyzed by SDS-PAGE. The gels were Coomassie brilliant blue stained (n = 3 independent replicates; results from 1 representative experiment are shown). (B) Intracellular proteases. L cell monolayers were infected with T1L, T1L μ1 M258I, T1L σ3 S344P, or T1L μ1 M258I σ3 S344P virions. At the indicated times post infection, the growth medium was supplemented with ammonium chloride. At 24 h post infection, the cells were lysed and viral yield was quantified by plaque assay. The data are presented as means ± SDs (n = 3 independent replicates). AC, ammonium chloride; Unt, untreated.

FIG 5 Thermostability of a T1L/T3D M2 variant. (A) Protein compositions. T1L/T3D M2 and T1L/T3D M2 μ1 M258I σ3 S344P virions and ISVPs were analyzed by SDS-PAGE. The gel was Coomassie brilliant blue stained. The migration of capsid proteins is indicated on the left. μ1 resolves as μ1C, and μ1δ resolves as δ (33). μ1N and Φ are too small to resolve on the gel (n = 3 independent replicates; results from 1 representative experiment are shown). (B) Size distribution profiles. T1L/T3D M2 or T1L/T3D M2 μ1 M258I σ3 S344P virions or ISVPs were analyzed by dynamic light scattering. For each variant, the virion (black) and ISVP (gray) size distribution profiles are overlaid (n = 3 independent replicates; results from 1 representative experiment are shown). (C) Thermal inactivation. T1L/T3D M2 or T1L/T3D M2 μ1 M258I σ3 S344P

679 virions or ISVPs were incubated in virus storage for 5 min at the indicated temperatures.
680 The change in infectivity relative to samples incubated at 4°C was determined by plaque
681 assay. The data are presented as means ± SDs. *, $P \leq 0.05$ and difference in change
682 in infectivity ≥ 2 $\log_{10}$ units (n = 3 independent replicates). (D) Degradation of σ3 by
683 exogenous protease. T1L/T3D M2 or T1L/T3D M2 μ1 M258I σ3 S344P virions were
684 incubated in virus storage buffer supplemented with endoproteinase LysC for the
685 indicated amounts of time at 37°C. Following digestion, equal particle numbers from
686 each time point were analyzed by SDS-PAGE. The gels were Coomassie brilliant blue
687 stained (n = 3 independent replicates; results from 1 representative experiment are
688 shown).
689
690 **FIG 6** Growth profiles of T1L and T1L/T3D M2 variants. (A and B) L cell monolayers
691 were infected with virions at an MOI of 10 PFU/cell or 0.01 PFU/cell. At the indicated
692 times post infection, the cells were lysed and viral yield was quantified by plaque assay.
693 The data are presented as means ± SDs. *, $P \leq 0.05$ and difference in viral yield ≥ 1
694 $\log_{10}$ unit (n = 3 independent replicates).

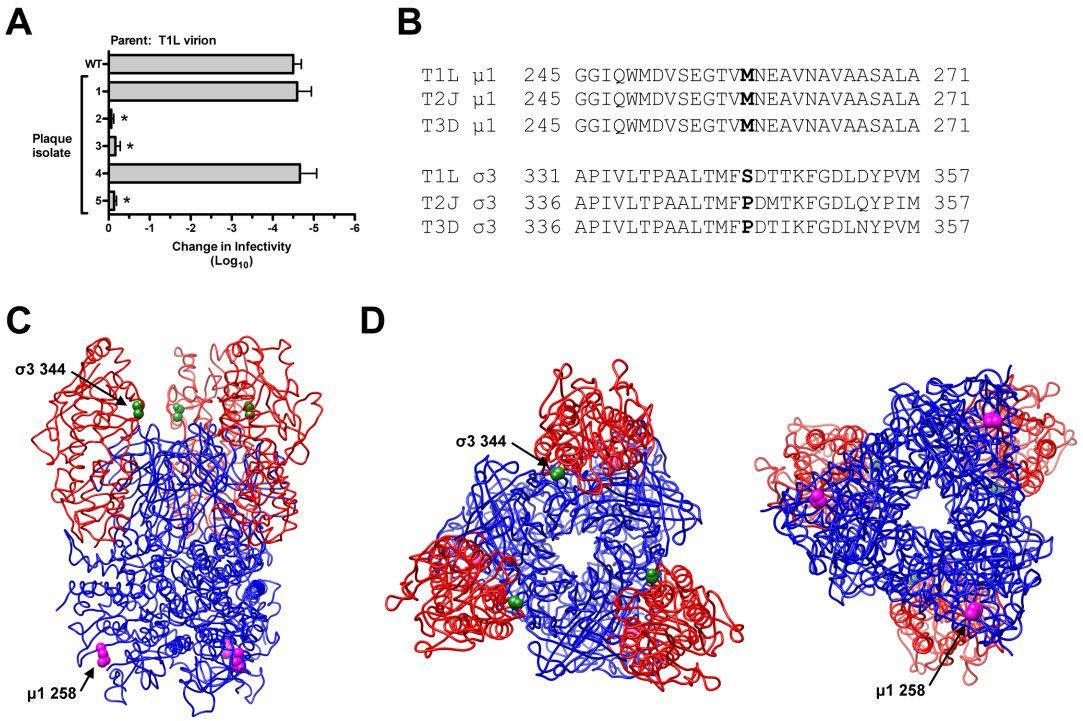

FIG 1 Selection, isolation, and sequencing of heat resistant strains. (A) Thermal inactivation. T1L virions were incubated for 5 min at 55°C. Surviving strains were plaque purified and amplified on L cells. To verify heat resistance, the infected cell lysates were incubated for 5 min at 55°C. The change in infectivity relative to samples incubated at 4°C was determined by plaque assay. The data are presented as means ± SDs. *, $P \leq 0.05$ and difference in change in infectivity ≥ 2 $\log_{10}$ units (n = 3 independent replicates). (B) Multiple sequence alignments. Residues corresponding to µ1 258 and σ3 344 are in boldface. (C) Side view of the T1L µ1-σ3 heterohexamer (7) (Protein Data Bank [PDB] accession number 1JMU). (D) Top and bottom views (left and right, respectively) of the T1L µ1-σ3 heterohexamer (7) (Protein Data Bank [PDB] accession number 1JMU). In panels C and D, µ1 monomers are colored blue, σ3 monomers are colored red, µ1 258 is represented by magenta spheres, and σ3 344 is represented by green spheres.

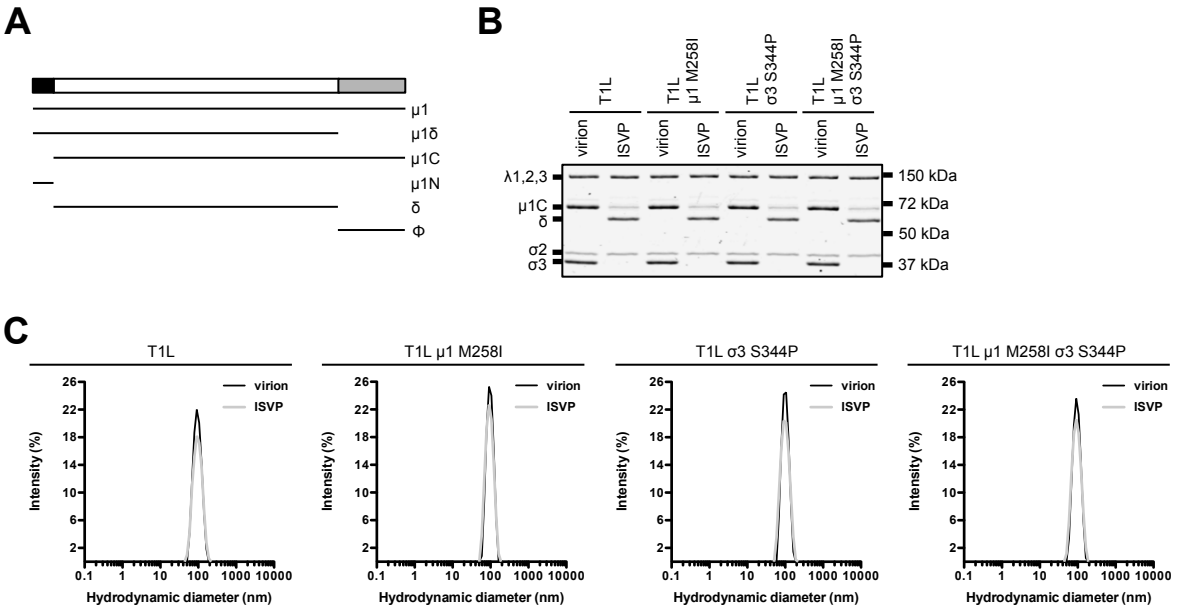

FIG 2 Protein compositions and size distribution profiles of T1L variants. (A) Schematic of μ1 cleavage fragments. (B) Protein compositions. T1L, T1L μ1 M258I, T1L σ3 S344P, and T1L μ1 M258I σ3 S344P virions and ISVPs were analyzed by SDS-PAGE. The gel was Coomassie brilliant blue stained. The migration of capsid proteins is indicated on the left. μ1 resolves as μ1C, and μ1δ resolves as δ (33). μ1N and Φ are too small to resolve on the gel (n = 3 independent replicates; results from 1 representative experiment are shown). (C) Size distribution profiles. T1L, T1L μ1 M258I, T1L σ3 S344P, or T1L μ1 M258I σ3 S344P virions or ISVPs were analyzed by dynamic light scattering. For each variant, the virion (black) and ISVP (gray) size distribution profiles are overlaid (n = 3 independent replicates; results from 1 representative experiment are shown).

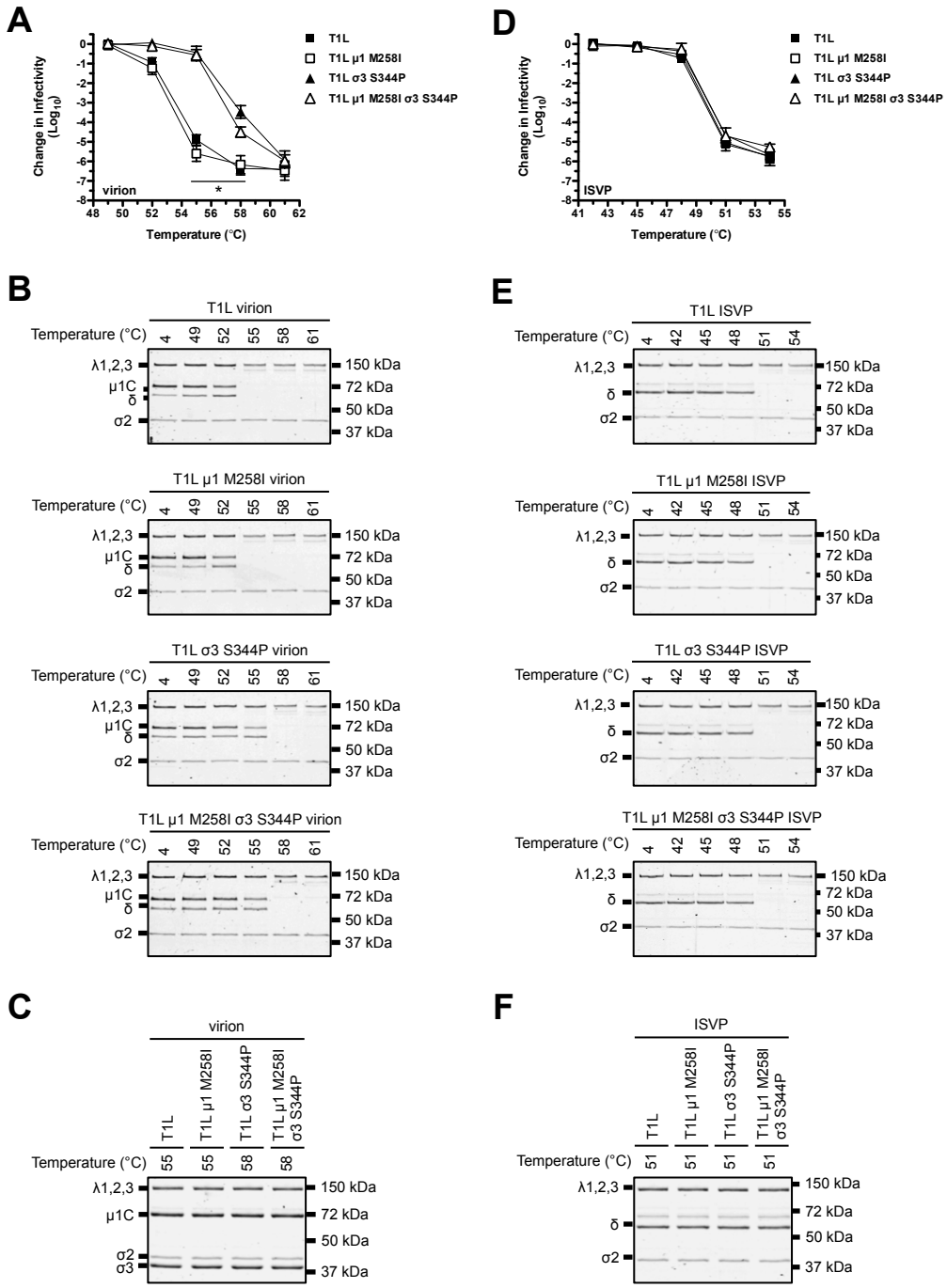

FIG 3 Thermostability of T1L variants. (A and D) Thermal inactivation. T1L, T1L µ1 M258I, T1L σ3 S344P, or T1L µ1 M258I σ3 S344P virions (A) or ISVPs (D) were incubated in virus storage for 5 min at the indicated temperatures. The change in infectivity relative to samples incubated at 4°C was determined by plaque assay. The data are presented as means ± SDs. *, $P \leq 0.05$ and difference in change in infectivity ≥ 2 $\log_{10}$ units (n = 3 independent replicates). (B and E) Heat induced conformational changes. T1L, T1L µ1 M258I, T1L σ3 S344P, or T1L µ1 M258I σ3 S344P virions (B) or ISVPs (E) were incubated in virus storage buffer for 5 min at the indicated temperatures. Each reaction was then treated with trypsin for 30 min on ice. Following digestion, equal particle numbers from each reaction were analyzed by SDS-PAGE. The gels were Coomassie brilliant blue stained (n = 3 independent replicates; results from 1 representative experiment are shown). (C and F). Composition of heated virus. T1L, T1L µ1 M258I, T1L σ3 S344P, or T1L µ1 M258I σ3 S344P virions (C) or ISVPs (F) were incubated in virus storage buffer for 5 min at the indicated temperatures. Equal particle numbers from each reaction were analyzed by SDS-PAGE. The gels were Coomassie brilliant blue stained (n = 3 independent replicates; results from 1 representative experiment are shown).

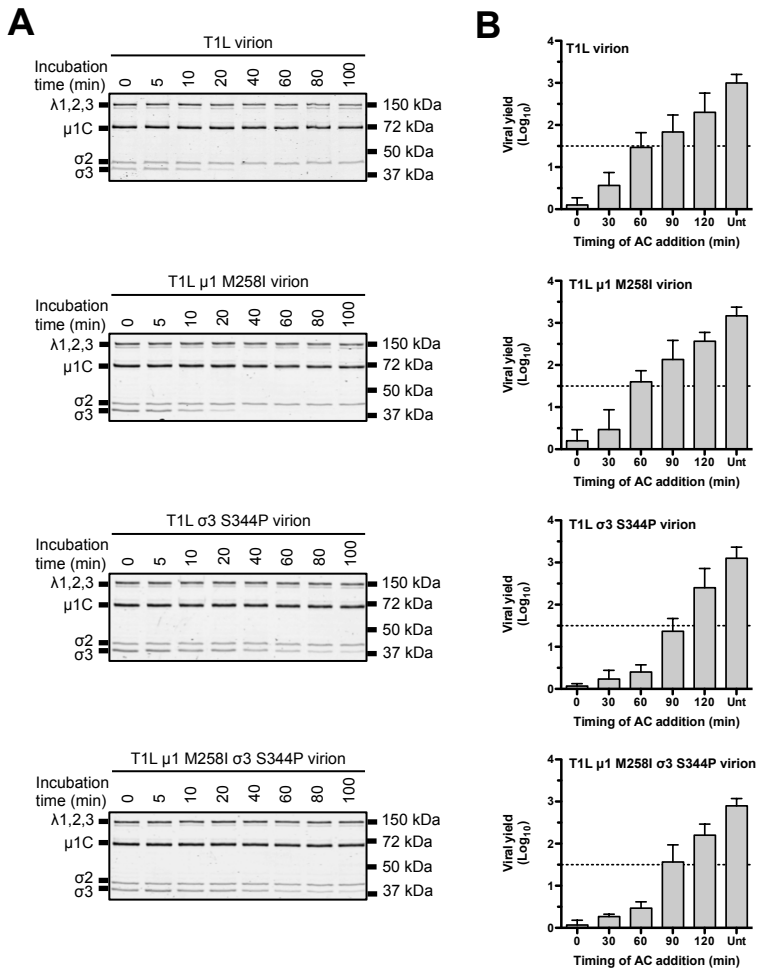

FIG 4 Degradation of σ3 by exogenous and intracellular proteases. (A) Exogenous protease. T1L, T1L μ1 M258I, T1L σ3 S344P, or T1L μ1 M258I σ3 S344P virions were incubated in virus storage buffer supplemented with endoproteinase LysC for the indicated amounts of time at 37°C. Following digestion, equal particle numbers from each time point were analyzed by SDS-PAGE. The gels were Coomassie brilliant blue stained (n = 3 independent replicates; results from 1 representative experiment are shown). (B) Intracellular proteases. L cell monolayers were infected with T1L, T1L μ1 M258I, T1L σ3 S344P, or T1L μ1 M258I σ3 S344P virions. At the indicated times post infection, the growth medium was supplemented with ammonium chloride. At 24 h post infection, the cells were lysed and viral yield was quantified by plaque assay. The data are presented as means ± SDs (n = 3 independent replicates). AC, ammonium chloride; Unt, untreated.

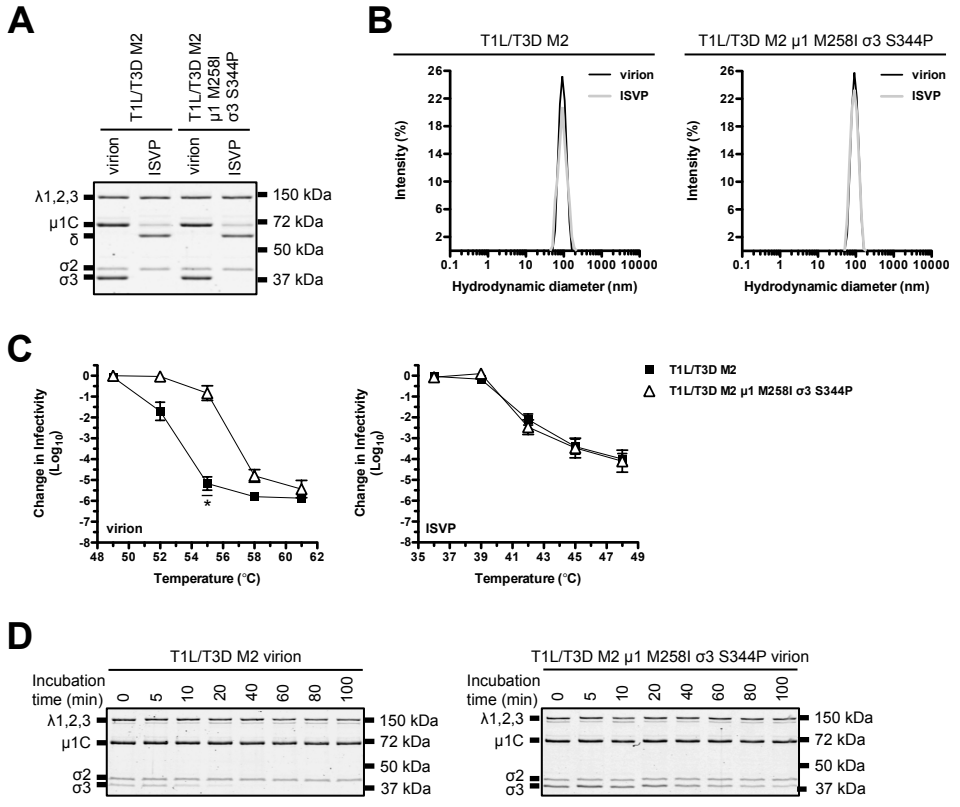

FIG 5 Thermostability of a T1L/T3D M2 variant. (A) Protein compositions. T1L/T3D M2 and T1L/T3D M2 μ1 M258I σ3 S344P virions and ISVPs were analyzed by SDS-PAGE. The gel was Coomassie brilliant blue stained. The migration of capsid proteins is indicated on the left. μ1 resolves as μ1C, and μ1δ resolves as δ (33). μ1N and Φ are too small to resolve on the gel (n = 3 independent replicates; results from 1 representative experiment are shown). (B) Size distribution profiles. T1L/T3D M2 or T1L/T3D M2 μ1 M258I σ3 S344P virions or ISVPs were analyzed by dynamic light scattering. For each variant, the virion (black) and ISVP (gray) size distribution profiles are overlaid (n = 3 independent replicates; results from 1 representative experiment are shown). (C) Thermal inactivation. T1L/T3D M2 or T1L/T3D M2 μ1 M258I σ3 S344P virions or ISVPs were incubated in virus storage for 5 min at the indicated temperatures. The change in infectivity relative to samples incubated at 4°C was determined by plaque assay. The data are presented as means ± SDs. *, $P \leq 0.05$ and difference in change in infectivity ≥ 2 $\log_{10}$ units (n = 3 independent replicates). (D) Degradation of σ3 by exogenous protease. T1L/T3D M2 or T1L/T3D M2 μ1 M258I σ3 S344P virions were incubated in virus storage buffer supplemented with endoproteinase LysC for the indicated amounts of time at 37°C. Following digestion, equal particle numbers from each time point were analyzed by SDS-PAGE. The gels were Coomassie brilliant blue stained (n = 3 independent replicates; results from 1 representative experiment are shown).

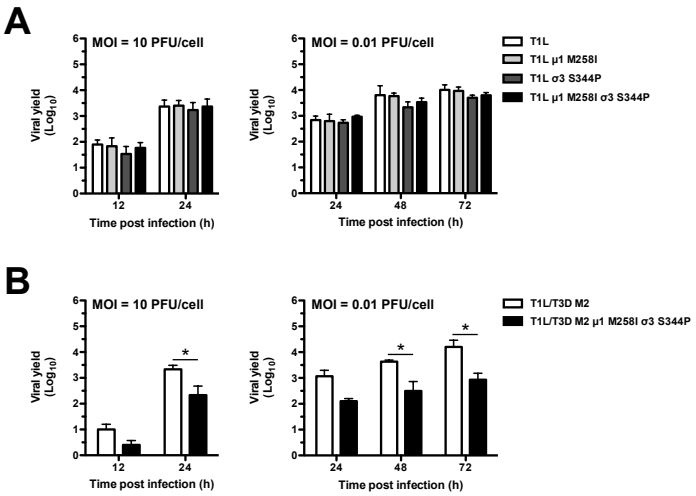

FIG 6 Growth profiles of T1L and T1L/T3D M2 variants. (A and B) L cell monolayers were infected with virions at an MOI of 10 PFU/cell or 0.01 PFU/cell. At the indicated times post infection, the cells were lysed and viral yield was quantified by plaque assay. The data are presented as means ± SDs. *, $P \leq 0.05$ and difference in viral yield ≥ 1 $\log_{10}$ unit (n = 3 independent replicates).